



## Modeling of ammonia combustion at low pressure

Catherine Duynslaegher<sup>a,\*</sup>, Francesco Contino<sup>a</sup>, Jacques Vandooren<sup>b</sup>, Hervé Jeanmart<sup>a</sup>

<sup>a</sup>Institute of Mechanics, Materials and Civil Engineering, Université catholique de Louvain, Place du Levant 2, 1348 Louvain la Neuve, Belgium

<sup>b</sup>Institute of Condensed Matter and Nanosciences, Université catholique de Louvain, Place Louis Pasteur 1, 1348 Louvain la Neuve, Belgium

### ARTICLE INFO

#### Article history:

Received 19 September 2011

Received in revised form 24 January 2012

Accepted 8 June 2012

Available online 30 June 2012

#### Keywords:

Ammonia combustion

Kinetic mechanism

Nitrogen oxides

### ABSTRACT

In the context of a hypothetical hydrogen based economy, ammonia has been suggested as a potential alternative to liquid fossil fuels for spark ignition (SI) engines. However, its use requires a detail understanding of its combustion characteristics, particularly the comprehension of the unavoidable thermal and fuel nitrogen oxides formation. This study presents the elaboration of an improved ammonia combustion mechanism validated for the flame structure prediction of ammonia, hydrogen, oxygen, argon flames investigated at several low pressures and for various conditions of equivalence ratio and of initial hydrogen content. The improved kinetic model is then reduced in order to be used in a complete SI engine numerical simulation. The comparison of the predictions of these mechanisms for the same ammonia flame structure is presented. The reduced mechanism contains 80 elementary reactions and 19 chemical species and allows a better understanding of the complete nitrogen oxides formation pathways.

© 2012 The Combustion Institute. Published by Elsevier Inc. All rights reserved.

### 1. Introduction

The problems of oil resources and CO<sub>2</sub> pollutant emissions becoming increasingly alarming, the search for alternatives to liquid fossil fuels is an important challenge for our society. Many studies are devoted to the evaluation of the energy efficiency and the environmental impact of alternative fuels. Among these, liquified petroleum gas, natural compressed gas, oxygenated fuels, bio-diesel and hydrogen (H<sub>2</sub>) have been put forward. Compressed or liquified hydrogen have been recognized as promising fuels. They can be produced from any raw energy source and can be environmentally friendly used in many prime movers (i.e. fuel cells [1], spark ignition (SI) engines [2], gas turbines [3], etc.). However, implementing a global hydrogen-based economy is not a currently feasible approach unless a suitable storage medium could be found [4]. Indeed, cost effectiveness due to challenges in storing and delivering compressed and cryogenic hydrogen are huge barriers to their near-term, wide-spread use. Therefore, to bypass such difficulties, the use of ammonia (NH<sub>3</sub>) in a modified SI engine has been suggested. Since hydrogen must still be produced to obtain ammonia in large amount, it can be seen as a hydrogen vector. Similar to hydrogen, ammonia can be used as a clean energy carrier and storage medium because it can potentially be burned in an environmentally benign way, exhausting only water and nitrogen. However, in practical uses, formation of thermal and fuel nitrogen oxides are unavoidable. Therefore, the successful application of ammonia as an alternative transportation fuel should be grounded

on a detailed understanding of its combustion characteristics. The elaboration of an appropriate combustion kinetic mechanism, based on experimental observations, is an important aspect in order to understand the way ammonia is decomposed and, maybe more importantly, the way the exhaust gases are formed.

Several ammonia combustion models have been proposed. The Bian et al. [5] model is specific to ammonia oxidation and has been tested on H<sub>2</sub>/O<sub>2</sub>/Ar flames seeded with ammonia and/or nitrogen monoxide (NO) and for ammonia flames burning in oxygen or in nitrogen monoxide [5–8]. The Lindstedt et al. [9] model is also specific to ammonia combustion and has been tested for the oxidation of ammonia in flat laminar premixed flames of H<sub>2</sub>/NH<sub>3</sub>/O<sub>2</sub>, NH<sub>3</sub>/NO/H<sub>2</sub>/O<sub>2</sub> and NH<sub>3</sub>/O<sub>2</sub>. The Konnov and De Ruyck [10] model is a complete H/N/O mechanism tested satisfactorily for decomposition, oxidation, ignition, and flame structure of ammonia but also of hydrogen, hydrazine, nitrous oxide, nitrogen monoxide and nitrogen dioxide. It is an integral part of the model developed for the combustion of small hydrocarbons (C<sub>1</sub>–C<sub>3</sub>) [11]. Similarly, the GRI [12] and the San Diego [13] models are used to simulate natural gas flames burning in oxygen or in air but take also into account nitrogenous species like ammonia, radical amidogen, and nitrogen monoxide. The flame structures obtained with these five mechanisms have been compared to experimental flame structures of eight ammonia–hydrogen flames [14]. The Cosilab software [15] has been used to perform the numerical simulations. The mechanisms of Lindstedt et al. [9], GRI [12] and San Diego [13] gave always results completely in disagreement with the experimental ones in terms of mole fraction gradients but also in terms of burned gases composition. The Bian et al. [5] model gave for all investigated flames underestimated values of the nitrogen

\* Corresponding author.

E-mail address: [catherine.duynslaegher@uclouvain.be](mailto:catherine.duynslaegher@uclouvain.be) (C. Duynslaegher).

monoxide concentration in the burned gases [16]. Since nitrogen monoxide is an important species to control in ammonia combustion, the reduced mechanism presented in this work has been elaborated on the Konnov and De Ruyck [10] model base. Indeed, for this model, most of the calculated mole fraction profiles agreed with the experimental ones but a significant divergence was observed for nitrous oxide ( $\text{N}_2\text{O}$ ) and amidogen radical ( $\text{NH}_2$ ). It was thus necessary to update kinetic parameters of the formation and degradation reactions of these species to obtain an improved mechanism leading to a better agreement with all the detected species [14]. When the original Konnov model has been established, only few measurements had been performed for ammonia combustion at low pressure and therefore, there were not enough experimental statements to justify a modification in rate constants. However, the experiments performed recently [14] justify to improve the Konnov mechanism for  $\text{N}_2\text{O}$  and  $\text{NH}_2$  simulation. Nevertheless, the original Konnov mechanism had been validated in shock tube for the peak mole fractions and times to peak mole fractions of  $\text{NH}$  and  $\text{NH}_2$  in the pyrolysis of  $\text{NH}_3$  diluted in argon at around 1 atm and temperatures between 2200 K and 3200 K [17]. It had also been validated for laminar flame speeds in  $\text{NH}_3$ – $\text{N}_2\text{O}$  mixtures at 70 torr and 60 °C [18], and ammonia–oxygen flames at atmospheric pressure [19–21] as summarized in [11].

The present work proposes the elaboration of an improved ammonia combustion mechanism validated for the flame structure prediction of eight ammonia/hydrogen flames. These flames have been investigated at different low pressures (60–120 mbar) using a molecular beam sampling coupled with a mass spectrometer, over a range of equivalence ratios ( $0.9 < \phi < 1.1$ ) and initial hydrogen percentages ( $5\% < X_{\text{H}_2} < 12.5\%$ ) [14]. The improved mechanism is also reduced in order to allow simulations in more practical cases, such as Computational Fluid Dynamics (CFDs) codes where the fluid mechanics aspects must also be taken into account and for which the diminution of the number of chemical species implied in the simulation is of a critical importance for the computational cost. This reduced mechanism allows a better understanding of the complete nitrogen oxides formation pathways which is of high importance when using ammonia as a fuel in SI engines.

## 2. Results and discussion

This section first presents the improvement of the Konnov ammonia combustion mechanism. It then describes the reduction of the improved model. Reaction numbering in the following discussion corresponds to reduced mechanism developed in the present work and available as [Electronic supplemental material](#).

### 2.1. Improvement of the Konnov mechanism

The Konnov mechanism overestimates the mole fraction profiles of  $\text{NH}_2$  and underestimates the ones of  $\text{N}_2\text{O}$ . To improve this mechanism, four reactions were modified according to the kinetic analysis of the main reactions involving these two chemical species. Tables 1 and 2 present the original and modified rate con-

**Table 2**

Rate constant modifications performed to improve  $\text{NH}_2$  prediction; \* = Estimated in this work; A ( $\text{cm}^3 \text{mol}^{-1} \text{s}^{-1}$ ),  $E_a$  (cal/mole).

	A	n	$E_a$	Ref.
1. $\text{NH}_2 + \text{H} = \text{NH} + \text{H}_2$	$6.3 \times 10^{13}$	0	8843	[42]
<b><math>\text{NH}_2 + \text{H} = \text{NH} + \text{H}_2</math></b>	<b><math>1 \times 10^6</math></b>	<b>2.32</b>	<b>799</b>	*
2. $\text{NH}_2 + \text{NH}_2 = \text{N}_2\text{H}_2 + \text{H}_2$	$10^{13}$	0	1500	[44]
<b><math>\text{NH}_2 + \text{NH}_2 = \text{N}_2\text{H}_2 + \text{H}_2</math></b>	<b><math>5 \times 10^{13}</math></b>	<b>0</b>	<b>1500</b>	*

stants of these reactions. The choice of the reaction rates which must be modified has been done on a contribution rates calculation and a sensitivity analysis. Then, the reaction rates have been modified in order to have a simulated profile within the experimental uncertainties of the experimental one [14]. Finally, the improved estimates of the reaction rates were based, depending on the reaction, on theoretical calculations or experimental values, while being in this case within the experimental uncertainties.

$\text{N}_2\text{O}$  maximum mole fraction being underestimated by the Konnov mechanism, the aim was thus to accelerate its formation and to slow down its degradation. A search in the literature [22–38] allowed to modify the kinetics parameters of these two reactions, in order to reach this goal. Reactions of imidogen ( $\text{NH}$ ) play a role in many aspects of nitrogen chemistry in combustion [32]. Perhaps most importantly, in the case of ammonia combustion, the reaction of  $\text{NH}$  with nitrogen monoxide is commonly known as the principal source of nitrous oxide ( $\text{N}_2\text{O}$ ). However, this reaction has two different possible routes:  $\text{NH} + \text{NO} \rightarrow \text{N}_2 + \text{OH}$  (49) or  $\text{NH} + \text{NO} \rightarrow \text{N}_2\text{O} + \text{H}$  (39). There are now many experimental and theoretical data focused on the determination of these rate constants. In general these fell into two categories, the measure of the overall rate constant,  $k_{49} + k_{39}$  [23–26] and the measure of the branching ratio of the two paths,  $f = k_{49}/(k_{49} + k_{39})$  [27–31], a parameter that is critical in predicting  $\text{N}_2\text{O}$  levels in combustion systems. Most of the overall rate constant measurements were performed at room temperature and there is a good agreement between the various results, ranging from  $2.3$  to  $3.5 \times 10^{13} \text{ cm}^3/\text{mol s}$  but to date the influence of temperature on this rate constant remains unclear. Moreover, there is significantly less agreement concerning the branching ratio between the two possible paths. In some experiments,  $\text{OH}$  was not detected at all, in others it was found to be the sole product. However, it is now accepted, following several independent measurements [30], that the yield of  $\text{N}_2 + \text{OH}$  is in the range of 5–30%. All of this shows that the rate constant of the path (39)  $\text{NH} + \text{NO} \rightarrow \text{N}_2\text{O} + \text{H}$  is not well known. Based on the most used rate constant calculated by Miller and Melius [28] ( $k_{39} = 2.3 \times 10^{14} [\text{cm}^3/\text{mol s}] T^{-0.4}$ ) and in order to accelerate the formation of  $\text{N}_2\text{O}$  to be in agreement with the experimental results [14], this rate constant has been estimated to be  $k_{39} = 5 \times 10^{14} [\text{cm}^3/\text{mol s}] T^{-0.4}$ . Figure 1 presents several experimental and theoretical rate constants found in the literature [9,12,22,28,32,39] together with the rate constant evaluated in this work (\*).

Concerning the reaction  $\text{N}_2\text{O} + \text{H} = \text{N}_2 + \text{OH}$  (60), Fig. 2 presents several experimental and theoretical rate constants found in the literature [22,33–38], showing that the exact value of this constant is not established but that an agreement has been reached concerning the global range of its value. Moreover, the kinetic data set in this work (\*) to slow down this reaction is in the range of those found in the literature.

For  $\text{NH}_2$  the problem is more complicated since this species is the main intermediate in the degradation of ammonia and thus also the precursor needed for the formation of approximately all the combustion products. As  $\text{NH}_2$  concentrations are overestimated by the Konnov mechanism but that the concentration profiles of main species appear to be correctly simulated [14], the consumption reactions of this species have to be accelerated. Based

**Table 1**

Rate constant modifications performed to improve  $\text{N}_2\text{O}$  prediction; \* = Estimated in this work; A ( $\text{cm}^3 \text{mol}^{-1} \text{s}^{-1}$ ),  $E_a$  (cal/mole).

	A	n	$E_a$	Ref.
1. $\text{NH} + \text{NO} = \text{N}_2\text{O} + \text{H}$	$2.5 \times 10^{16}$	−1.03	835	[22]
<b><math>\text{NH} + \text{NO} = \text{N}_2\text{O} + \text{H}</math></b>	<b><math>5 \times 10^{14}</math></b>	<b>−0.4</b>	<b>0</b>	*
2. $\text{N}_2\text{O} + \text{H} = \text{N}_2 + \text{OH}$	$2.2 \times 10^{14}$	0	16750	[22]
<b><math>\text{N}_2\text{O} + \text{H} = \text{N}_2 + \text{OH}</math></b>	<b><math>5 \times 10^{13}</math></b>	<b>0</b>	<b>15200</b>	*

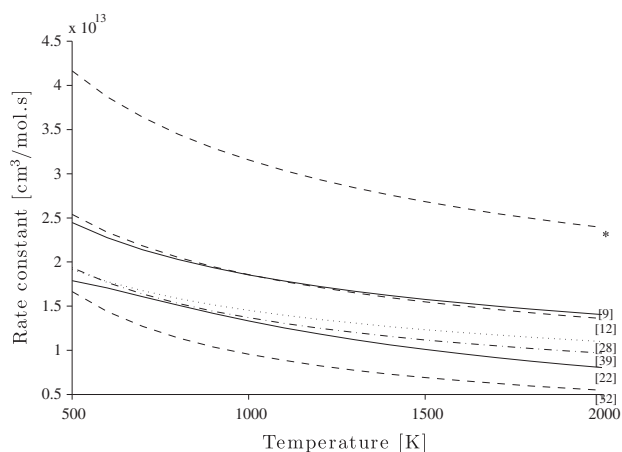


Fig. 1. Rate constants of the reaction  $\text{NH} + \text{NO} = \text{N}_2\text{O} + \text{H}$ .

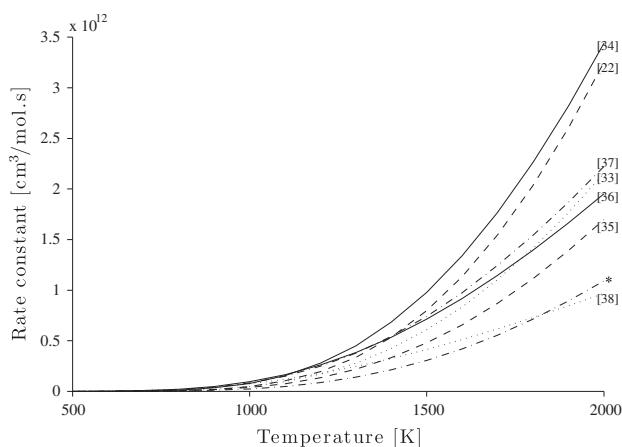


Fig. 2. Rate constants of the reaction  $\text{N}_2\text{O} + \text{H} = \text{N}_2 + \text{OH}$ .

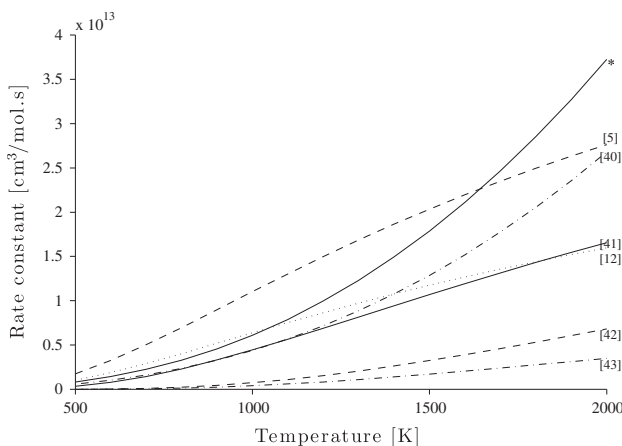


Fig. 3. Rate constants of the reaction  $\text{NH}_2 + \text{H} = \text{NH} + \text{H}_2$ .

on the rate analysis of the main reaction pathways of  $\text{NH}_2$  consumption, the kinetic parameters of reactions presented in Table 2 have been adjusted to avoid a large impact on other species like  $\text{H}_2\text{O}$ ,  $\text{N}_2$  or  $\text{NO}$  correctly reproduced by the simulation.

The rate constant of reaction  $\text{NH}_2 + \text{H} = \text{NH} + \text{H}_2$  (21) suggested in the theoretical work of Linder et al. [40] improved the numerical simulation of  $\text{NH}_2$  profile. This constant has been further adjusted

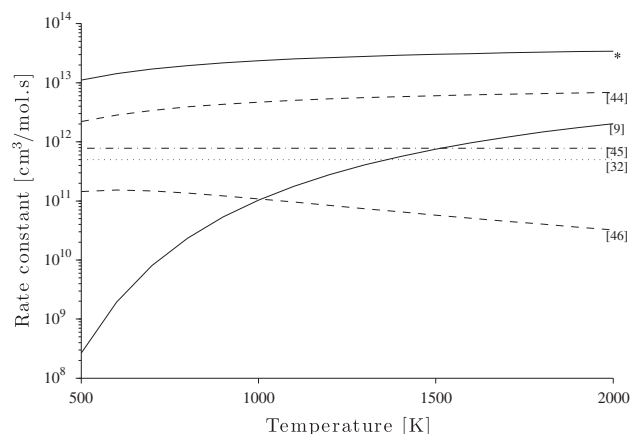


Fig. 4. Rate constants of the reaction  $\text{NH}_2 + \text{NH}_2 = \text{N}_2\text{H}_2 + \text{H}_2$ .

in order to fit experimental  $\text{NH}_2$  profiles [14]. Figure 3 presents several experimental and theoretical rate constants found in the literature [5,12,40–43] together with the rate constant estimated in this work (\*).

Concerning the reaction  $\text{NH}_2 + \text{NH}_2 = \text{N}_2\text{H}_2 + \text{H}_2$  (25), as presented in Fig. 4 its rate constant is only estimated and there are few references in the literature [9,32,44–46]. The Konnov mechanism ( $k = 10^{13} [\text{cm}^3/\text{mol.s}] \times \exp(-1500 [\text{cal/mole}]/\text{RT})$ ) [44] suggests an estimated value based on the work of Stothard et al. [45] performed at low pressure but at room temperature. Therefore, this rate constant has been adjusted to  $k = 5 \times 10^{13} [\text{cm}^3/\text{mol.s}] \times \exp(-1500 [\text{cal/mole}]/\text{RT})$  in order to fit experimental  $\text{NH}_2$  profiles [14].

The modified Konnov mechanism is validated at low pressure for the simulation of the structure of all the flames investigated previously by Duynslaegher et al. [14]. To illustrate this validation, mole fraction profiles obtained with the original Konnov mechanism and with the modified Konnov mechanism are compared in Figs. 5–8 for an ammonia–oxygen–hydrogen flame stabilized at 50 mbar ( $\phi = 1.02$ , 24%  $\text{NH}_3$ , 7.5%  $\text{H}_2$ , 21.3%  $\text{O}_2$ , 47.2% Ar). Concerning the major species, i.e. ammonia, oxygen, nitrogen, water and argon, they are all well simulated by both mechanisms (Fig. 5).

For the minor species (Figs. 6–8), the experimentally detected ones were also well reproduced by the Konnov mechanism, excepted nitrous oxide and the amidogen radical for which the predictions have been significantly improved when using the modified Konnov mechanism.

Finally, the non detected minor species are similarly simulated by both mechanisms excepted  $\text{N}_2\text{H}_2$  and  $\text{N}$ . The comparison of the formation and consumption kinetic pathways for the two mechanisms can help to understand these differences. Those ones are depicted in Figs. 9–12. These diagrams represent the weight of the reactions on the global formation or consumption of a species. Since the several pathways involved in the formation of a species do not necessarily correspond to the pathways involved in its consumption, these diagrams must therefore be read separately. The main objective of Figs. 9–12 is to present the nitrogen monoxide formation and consumption pathways. In both mechanisms, this species is formed mainly from  $\text{HNO}$ ,  $\text{NH}$  oxidation or  $\text{NO}_2$  equilibrium and consumed by the  $\text{NO}_2$  equilibrium and to form nitrogen.

$\text{N}_2\text{H}_2$  is formed in both mechanisms mainly by the reaction  $\text{NH}_2 + \text{NH}_2 \rightarrow \text{N}_2\text{H}_2 + \text{H}_2$  (25), reaction that has been accelerated in the model presented in this work in order to increase the  $\text{NH}_2$  consumption. This explains why this species is present in much higher quantities in the modified model.

The increase in the  $\text{N}$  radical concentration comes from the global changes in term of nitrogenous species applied to the Konnov mechanism.

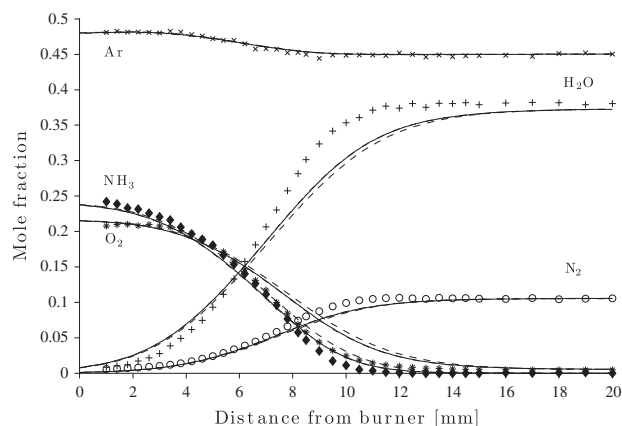


**Fig. 5.** Comparison of the Konnov, modified Konnov and reduced mechanisms for the structure prediction of major species. Symbols: experiments [14], solid lines: modified Konnov mechanism, dashed lines: Konnov mechanism [10], dash-dotted lines: reduced mechanism. Flame composition: 24%  $\text{NH}_3$ , 7.5%  $\text{H}_2$ , 21.3%  $\text{O}_2$  and 47.2%  $\text{Ar}$ .

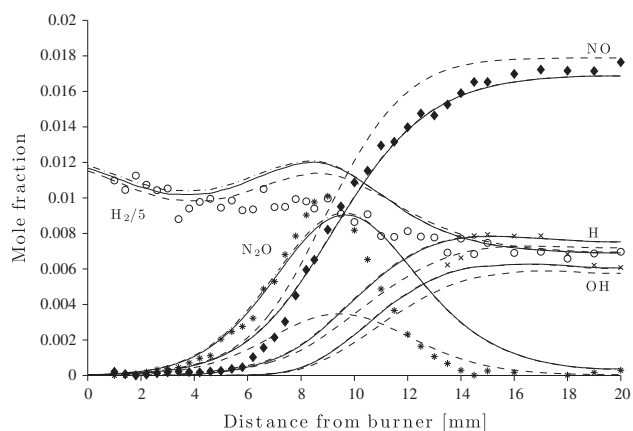


**Fig. 6.** Comparison of the Konnov, modified Konnov and reduced mechanisms for the structure prediction of some minor species ( $1.5 \times 10^{-3} < X_i < 2 \times 10^{-2}$ ). Symbols: experiments [14], solid lines: Modified Konnov mechanism, dashed lines: Konnov mechanism [10], dash-dotted lines: reduced mechanism.

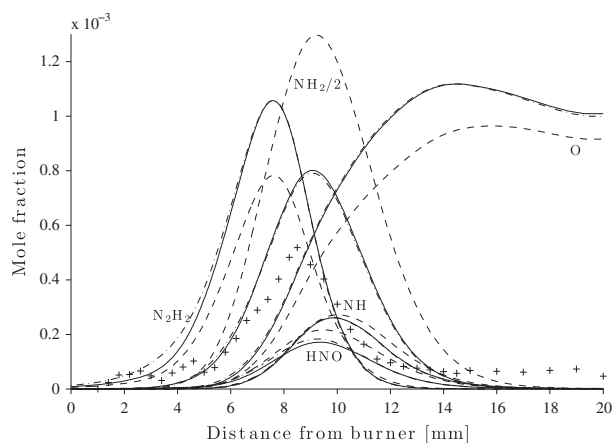


**Fig. 7.** Comparison of the Konnov, modified Konnov and reduced mechanisms for the structure prediction of some minor species ( $1 \times 10^{-4} < X_i < 1.5 \times 10^{-3}$ ). Symbols: experiments [14], solid lines: modified Konnov mechanism, dashed lines: Konnov mechanism [10], dash-dotted lines: reduced mechanism.

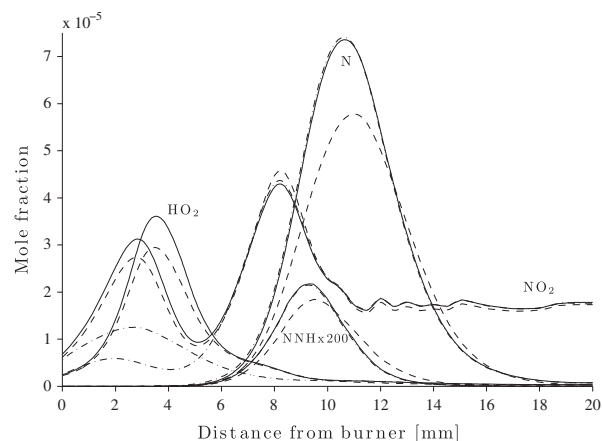


**Fig. 8.** Comparison of the Konnov, modified Konnov and reduced mechanisms for the structure prediction of some minor species ( $X_i < 1 \times 10^{-4}$ ). Solid lines: modified Konnov mechanism, dashed lines: Konnov mechanism [10], dash-dotted lines: reduced mechanism.

The unusual aspect of the  $\text{NO}_2$  profile comes from the several reactions involved in its formation and consumption. Indeed, this species is formed in the Konnov mechanism and in the modified Konnov mechanism by the reactions  $\text{NH}_2 + \text{HONO} = \text{NO}_2 + \text{NH}_3$  (not present in the reduced mechanism),  $\text{NO} + \text{HO}_2 = \text{NO}_2 + \text{OH}$  (64) and  $\text{NO} + \text{O} (+\text{M}) = \text{NO}_2 (+\text{M})$  (53) and consumed by the reaction  $\text{NO}_2 + \text{H} = \text{NO} + \text{OH}$  (63). Reaction (64) takes place in the first part of the flame, near the burner surface, while the consumption reaction (63) begins around 3 mm from the burner surface and explains the first peak observed in the mole fraction profile. Then reactions  $\text{NH}_2 + \text{HONO} = \text{NO}_2 + \text{NH}_3$  and (53) take place in the second part of the flame, in the flame front, and allow to explain the second peak observed at a distance of 8 mm from the burner surface. Finally, reactions (53) and (63) remain important in the burned gases and allow to explain the residual  $\text{NO}_2$  mole fraction in the burned gases.

## 2.2. Reduction of the improved kinetic mechanism

To reduce the size of the validated modified Konnov mechanism, a contribution rates calculation has been performed with the Cosilab software [15] for all the low pressure investigated flames presented by Duynslaegher et al. [14]. A contribution rates calculation allows to find the reactions which are the most important for the formation or the consumption of each species in the flame. In a mechanism such the one of Konnov which has been established to be used for several fuels in several conditions, a lot of reactions are added to be sure to have the more complete version of the mechanism. However, to have a mechanism only for ammonia combustion some species and some reactions presented in the Konnov mechanism can be removed. To know which reaction is important or not, a contribution rates calculation is thus performed. The result of this analysis showed that only 143 reactions contribute for at least 1% in the formation or the consumption of at least one chemical species. The same rate analysis has then been performed with the modified Konnov mechanism for laminar, freely propagating premixed flames burning at atmospheric pressure and room temperature at equivalence ratios of 0.5, 1 and 1.5. Consequently, 18 reactions have been added to the 143 first one. Finally, this freely propagating flame has been simulated for the same equivalence ratios but for higher pressure and temperature conditions corresponding to a spark ignition compression ratio of 20 needed for an efficient ammonia–air combustion ( $T \approx 830 \text{ K}$ ;  $P \approx 55 \text{ atm}$ ) [47]. These last simulations showed that

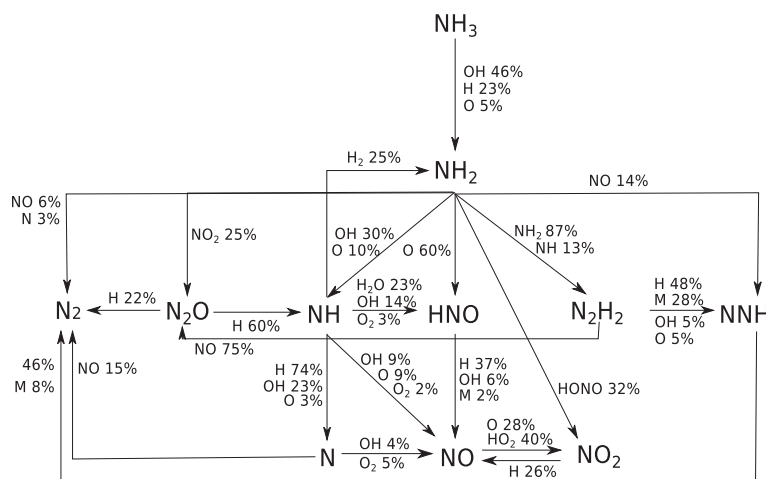


Fig. 9. Formation reaction pathways for the modified Konnov mechanism.

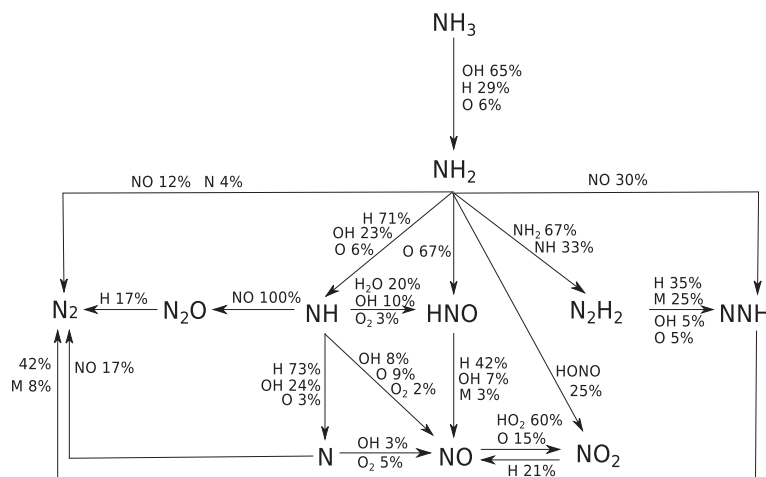


Fig. 10. Formation reaction pathways for the Konnov mechanism.

10 reactions had to be added to the previous ones, giving a set of 171 reactions involving 31 species. Then, in order to decrease the number of chemical species, those present in very small quantities ( $X_i < 10^{-8}$ ) and not necessary for the formation or consumption of main species, namely,  $N_2O_3$ ,  $NO_3$ ,  $HONO$ ,  $HNO_3$ ,  $N_2O_4$ ,  $HNNO$ ,  $N_2H_3$ ,  $N_2H_4$ ,  $H_2NO$ ,  $HNOH$ ,  $NH_2OH$  and  $H_2O_2$ , together with the corresponding reactions involving only these species, were removed to obtain the reduced mechanism containing 80 reactions and 19 chemical species. The mechanism has been reduced by keeping in mind the possibility of the use of ammonia in a spark ignition engine and therefore performing simulations at atmospheric pressure and at highest pressure and temperature such as those encountered in a SI engine. The aim was to obtain results in agreement with those reached with the original Konnov mechanism since only two species were not correctly reproduced by this mechanism but that globally the mechanism was not bad at all. 80 reactions is the minimum needed to avoid any changes in any conditions simulated. This reduced kinetic mechanism has been tested at low pressure for the simulations of the structure of all flat flames investigated previously by Duynslaegher et al. [14]. For example, the results of this reduced mechanism for the simulation of the flame structure together with the comparison with those coming from the modified Konnov mechanism are depicted in Figs.

5–8 for an ammonia–oxygen–hydrogen flame stabilized at 50 mbar [14] ( $\phi = 1.02$ , 24%  $NH_3$ , 7.5%  $H_2$ , 21.3%  $O_2$ , 47.2% Ar).

Concerning main species, i.e., ammonia, oxygen, nitrogen, water and argon, the reduction of the modified Konnov mechanism does not lead to any change in their predictions (Fig. 5). For the minor species (Figs. 6–8), their predictions are identical for both mechanisms excepted for  $NO_2$  and  $HO_2$ . The comparison of the formation and consumption kinetic pathways for the two mechanisms can help to understand these differences. In the modified Konnov mechanism,  $NO_2$  is formed thanks to the three reactions presented in the previous Section 2.1 while it is only produced by reaction (53) in the reduced model since  $HONO$  is not taken into consideration in this mechanism and  $HO_2$  mole fraction is strongly lowered. Reaction (64) produces  $NO_2$  mainly in the first part of the flame where the temperature is lower and explains the difference in the  $NO_2$  profile between the two mechanisms. The persistence of  $NO_2$  in the burned gases, which is observed in the Konnov mechanism, in the modified Konnov mechanism and in the reduced mechanism, can be explained by its equilibrium with  $NO$ . Indeed,  $NO_2$  is produced mainly by reaction (64) in the Konnov and the modified Konnov mechanism and by reaction (53) in the reduced mechanism while it is consumed mainly by the reaction  $NO_2 + H = NO + OH$  (63) in the three mechanisms. All of these



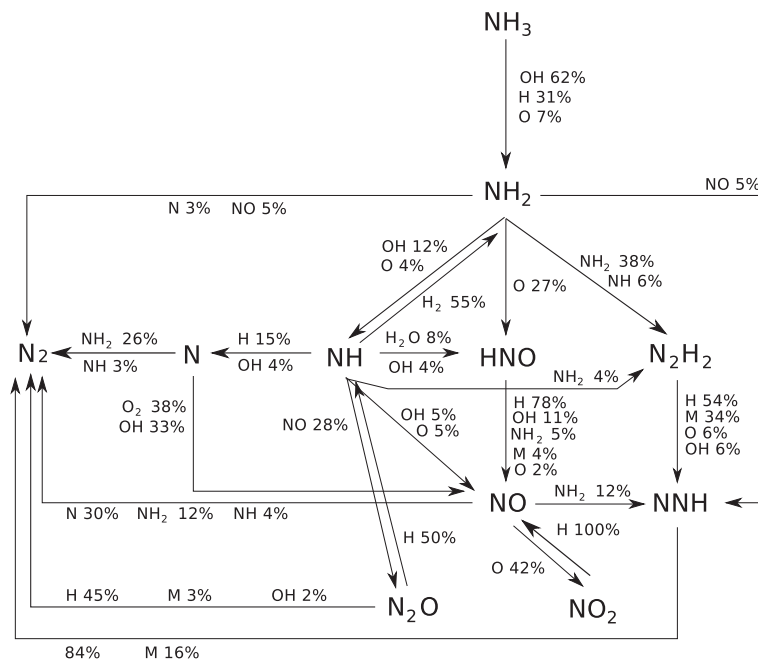


Fig. 11. Consumption reaction pathways for the modified Konnov mechanism.

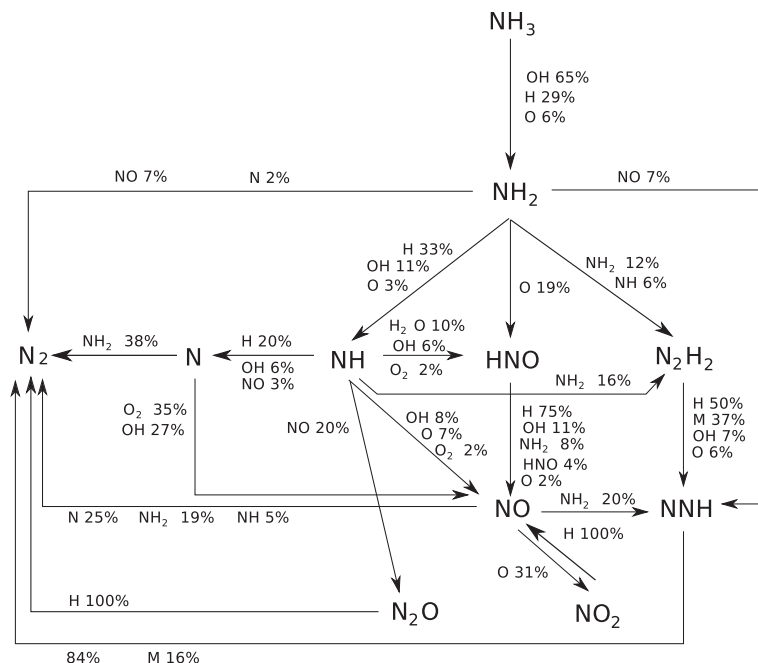


Fig. 12. Consumption reaction pathways for the Konnov mechanism.

reactions suggest an equilibrium with the nitrogen monoxide which is persistent in the burned gases. Finally,  $\text{HO}_2$  is formed in both mechanisms by the reaction  $\text{H} + \text{O}_2 + \text{M} = \text{HO}_2 + \text{M}$  (6), mainly in the first part of the flame front and consumed mainly by the reaction  $\text{H} + \text{HO}_2 = \text{OH} + \text{OH}$  (13). The increase of the consumption reaction speed and the decrease of the formation reaction speed in the reduced mechanism compared to the modified Konnov mechanism explain the reduction of the  $\text{HO}_2$  mole fraction in the reduced mechanism.

The original Konnov model and the reduced mechanism presented in this work have also been validated for laminar flame speed predictions of ammonia–air flames at atmospheric pressure

[48]. These two mechanisms gave results in agreement with the experimental measurements, reaching a peak laminar burning velocity of  $14 \text{ cm s}^{-1}$  around stoichiometric conditions. The predictions obtained with the Konnov mechanism and the reduced one have also been compared to laminar flame speed measurements of ammonia–oxygen mixtures at 70 mm Hg presented by Andrews and Gray [49]. Under stoichiometric conditions, the experimental value is equal to  $110 \text{ cm s}^{-1}$  and the simulated ones are equal to  $146 \text{ cm s}^{-1}$  and  $142 \text{ cm s}^{-1}$  for the reduced and the Konnov mechanism respectively. The modifications made to the original Konnov mechanism does thus not have any impact on such low pressure laminar flame speed predictions.

### 3. Conclusion

This work has presented an improved reduced mechanism for ammonia combustion validated for the flame structure prediction of ammonia, hydrogen, oxygen, argon flames investigated at several low pressures and for various conditions of equivalence ratio and of initial hydrogen content [14]. This kinetic model is based on the one proposed by Konnov and De Ruyck [10] and the simulation of  $\text{NH}_2$  and  $\text{N}_2\text{O}$  has been improved. The comparison of the predictions of these mechanisms for the same ammonia flame has been presented indicating a better simulation of the experimental results with the improved ammonia combustion mechanism. The improved mechanism has then been reduced in order to be used, at lower computational cost, in CFD simulations of spark ignition engines. This kinetic model contains 80 elementary reactions and 19 chemical species and allows a better understanding of the complete nitrogen oxides formation pathways which is of high importance when using ammonia as a fuel in spark ignition engines.

### Acknowledgements

C. Duynslaegher is grateful to the F.R.S. – FNRS for the financial support of her Ph.D. Thesis.

### Appendix A. Supplementary material

Supplementary data associated with this article can be found, in the online version, at <http://dx.doi.org/10.1016/j.combustflame.2012.06.003>.

### References

- [1] D. Hotza, J.D. da Costa, *Int. J. Hydrogen Energy* 33 (2008) 4915–4935.
- [2] C. Rakopoulos, G. Kosmadakis, J. Demuynck, M. de Paepe, S. Verhelst, *Int. J. Hydrogen Energy* 36 (2011) 5163–5180.
- [3] P. Gobatto, M. Masi, A. Toffoio, A. Lazzaretto, *Int. J. Hydrogen Energy* 36 (2011) 7993–8002.
- [4] J. Ritter, A. Ebner, J. Wang, R. Zidan, *Mater. Today* 6 (2003) 18–23.
- [5] J. Bian, J. Vandooren, P. van Tiggelen, *Proc. Combust. Inst.* 23 (1990) 379–386.
- [6] J. Vandooren, J. Bian, P. van Tiggelen, *Combust. Flame* 98 (1994) 402–410.
- [7] J. Vandooren, *Combust. Sci. Technol.* 84 (1992) 335–344.
- [8] J. Bian, J. Vandooren, P. van Tiggelen, *Proc. Combust. Inst.* 21 (1986) 953–963.
- [9] R. Lindstedt, F. Lockwood, M. Selim, *Combust. Sci. Technol.* 99 (1994) 253–276.
- [10] A. Konnov, J. De Ruyck, *Combust. Sci. Technol.* 168 (2001) 1–46.
- [11] A. Konnov, *Combust. Flame* 156 (2009) 2093–2105.
- [12] G. Smith, D. Golden, M. Frenklach, N. Moriarty, B. Eiteneer, M. Goldenberg, C. Bowman, R. Hanson, S. Song, J.W.C. Gardiner, V. Lissianski, Z. Qin, 1999, [www.me.berkeley.edu/gri\\_mech](http://www.me.berkeley.edu/gri_mech).
- [13] The Combustion Division of the Center for Energy Research at the University of California, 2005, [www.mae.ucsd.edu/combustion/cermech](http://www.mae.ucsd.edu/combustion/cermech).
- [14] C. Duynslaegher, H. Jeanmart, J. Vandooren, *Proc. Combust. Inst.* 32 (2009) 1277–1284.
- [15] Cosilab, Rotexo GmbH and Co. KG, Haan, Germany, 2007, [www.rotexo.com](http://www.rotexo.com).
- [16] C. Duynslaegher, H. Jeanmart, J. Vandooren, *Combust. Sci. Technol.* 181 (2009) 1092–1106.
- [17] D.F. Davidson, K. Kohse-Hoinghaus, A.Y. Chang, R.K. Hanson, *Int. J. Chem. Kinet.* 22 (1990) 513–535.
- [18] M. Brown, D. Smith, *Proc. Combust. Inst.* 25 (1994) 1011–1018.
- [19] R. Murray, A. Hall, *Trans. Faraday Soc.* 47 (1951) 743–751.
- [20] L. Cohen, *Fuel* 34 (1955) 123–127.
- [21] V. Zakaznov, L. Kursheva, *Zh. Prikl. Khim.* 53 (1980) 1865–1867.
- [22] J. Bozzelli, A. Chang, A. Dean, *Proc. Combust. Inst.* 25 (1994) 965–974.
- [23] W. DeMore, S. Sander, D. Golden, R. Hampson, M. Kurylo, C. Howard, A. Ravishankara, C. Kolb, M. Molina, *JPL Publ.* 97–94 (1997) 1–266.
- [24] H. Lillich, A. Schuck, H. Volpp, J. Wolfrum, *Proc. Combust. Inst.* 25 (1994) 993–1001.
- [25] W. Hack, H. Wagner, A. Zaspkyin, *Ber. Bunsen Ges. Phys. Chem.* 98 (1994) 156–164.
- [26] K. Yokoyama, Y. Sakane, T. Fueno, *Bull. Chem. Soc. Jpn.* 64 (1991) 1738–1742.
- [27] S. Okada, A. Tezaki, A. Miyoshi, H. Matsui, *J. Chem. Phys.* 101 (1994) 9582–9588.
- [28] J. Miller, C. Melius, *Proc. Combust. Inst.* 24 (1992) 719–726.
- [29] H. Szichman, M. Baer, H. Volpp, J. Wolfrum, *J. Phys. Chem. A* 102 (1998) 10455–10459.
- [30] H. Szichman, M. Baer, *J. Chem. Phys.* 105 (1996) 10380–10386.
- [31] M. Simonson, K. Bradley, G. Schatz, *Chem. Phys. Lett.* 244 (1995) 19–26.
- [32] J. Miller, C. Bowman, *Prog. Energy Combust. Sci.* 15 (1989) 287–338.
- [33] W. Tsang, J. Herron, *J. Phys. Chem. Ref. Data* 20 (1991) 609–663.
- [34] Y. Hidaka, H. Takuma, M. Suga, *Bull. Chem. Soc. Jpn.* 58 (1985) 2911–2916.
- [35] R. Hanson, S. Salimian, *Combustion Chemistry*, Springer, Verlag, New York, 1984.
- [36] H. Henrici, S. Bauer, *J. Chem. Phys.* 50 (1969) 1333–1342.
- [37] V. Balakhnine, J. Vandooren, P. van Tiggelen, *Combust. Flame* 28 (1977) 165–173.
- [38] G. Dixon-Lewis, M. Sutton, A. Williams, *Proc. Combust. Inst.* 10 (1965) 495–502.
- [39] J.A. Miller, M.D. Smooke, R.M. Green, R.J. Kee, *Combust. Sci. Technol.* 34 (1983) 149–176.
- [40] D. Linder, X. Duan, M. Page, *J. Phys. Chem.* 99 (1995) 11458–11463.
- [41] J. Dove, W. Nip, *Can. J. Chem.* 57 (1979) 689–701.
- [42] M. Rohrig, H. Wagner, *Proc. Combust. Inst.* 25 (1994) 975–981.
- [43] M. Yumura, T. Asaba, *Proc. Combust. Inst.* 18 (1981) 863–872.
- [44] A.A. Konnov, J. De Ruyck, *Combust. Flame* 124 (2001) 106–126.
- [45] N. Stothard, R. Humpfer, H. Grotheer, *Chem. Phys. Lett.* 240 (1995) 474–480.
- [46] O. Skreiberg, P. Kilpinen, P. Glarborg, *Combust. Flame* 136 (2004) 501–518.
- [47] C. Duynslaegher, H. Jeanmart, J. Vandooren, *Fuel* 89 (2010) 3540–3545.
- [48] C. Duynslaegher, Experimental and numerical study of ammonia combustion, PhD Thesis, Université catholique de Louvain, Belgium, 2011. <http://hdl.handle.net/2078.1/89103>.
- [49] D. Andrews, P. Gray, *Combust. Flame* 8 (1964) 113–126.